

# Optimization of Activated Carbons Prepared from *Parinari macrophylla* Shells

Maâzou Siragi D. B.<sup>1\*</sup>, Didier Desmecht<sup>2</sup>, Halidou I. Hima<sup>1</sup>, Ousmaila Sanda Mamane<sup>3</sup>, Ibrahim Natatou<sup>1</sup>

<sup>1</sup>Materials Water and Environment Laboratory, Sciences and Technologies Faculty, Abdou Moumouni University, Niamey, Niger

<sup>2</sup>LABIRIS, Physical Chemistry and Catalysis, Brussels, Belgium

<sup>3</sup>Sciences and Technologies Faculty, Agadez University, Agadez, Niger

Email: \*siragi\_maazou@yahoo.fr

**How to cite this paper:** Siragi D. B., M., Desmecht, D., Hima, H.I., Mamane, O.S. and Natatou, I. (2021) Optimization of Activated Carbons Prepared from *Parinari macrophylla* Shells. *Materials Sciences and Applications*, 12, 207-222.

<https://doi.org/10.4236/msa.2021.125014>

**Received:** March 27, 2021

**Accepted:** May 14, 2021

**Published:** May 17, 2021

Copyright © 2021 by author(s) and Scientific Research Publishing Inc.

This work is licensed under the Creative

Commons Attribution International

License (CC BY 4.0).

<http://creativecommons.org/licenses/by/4.0/>



Open Access

## Abstract

Plant matter constitutes an important source for producing carbonaceous materials. This work deals with the preparation of active carbons from shells of *Parinari macrophylla* (agricultural waste in Niger). Physical, chemical and mixed activations are considered. Several parameters of preparation are optimized, as the nature of the activation gas (N<sub>2</sub> or CO<sub>2</sub>, dry and wet), the concentration of the activating agent (H<sub>3</sub>PO<sub>4</sub>), the time of impregnation and the pyrolysis temperature program. The active carbons are characterized through their iodine numbers, their specific surface areas and their porous volumes. Active carbons, produced from shells of *Parinari macrophylla* display iodine numbers up to 599 mg I<sub>2</sub>/g and specific surface areas up to 727 m<sup>2</sup>/g. They also show microporous characteristics, with a mean pore diameter, usually, lower than 20 Å and a microporous surface percentage up to 88.7% and a microporous volume percentage up to 82.1%. The microporosity is far more developed for the active carbons produced by chemical activation.

## Keywords

Biomass, *Parinari macrophylla*, Pyrolysis, Optimization, Active Carbon

## 1. Introduction

The valorization of natural resources is a growing aspect of today's research. Food industries and the consumption of an ever-growing population produce a huge amount of agricultural wastes that are not without consequences on the environment. Due to their high carbon content, these wastes can be valorized as raw materials for the production of active carbons (A.C.). Any lignocellulosic biomass can be turned into active carbon through a thermal treatment of pyro-

lysis and activation. This activation can be physical (use of gases as  $N_2$ ,  $CO_2$ , ...) and/or chemical (use of activating agent solutions of  $H_3PO_4$ ,  $H_2SO_4$ ,  $KOH$ ,  $ZnCl_2$ , ...). Physical activation needs to be carried out at higher temperatures (800°C to 1000°C [1] [2] [3] [4]), but the active carbons, synthesized that way, are free from impurities left by the activating agents used in chemical activations [5] [6] [7] [8]. Thus, meeting the requirements of sustainable development, active carbons are produced from agricultural by-products, such as coconut shells [5] [6], date stones [2], coffee grounds [8], *Balanites aegyptiaca* shells [7], sugarcane bagasse and sunflower seed hulls [9].

Several works have already studied the production and the characterization (specific surface areas, pores size distributions, crystalline state, surface functions) of A.C. from various biomasses [1] [2] [3] [4] [5] [8] [9] [10] [11] [12]. These characteristics are important for the use of A.C. as adsorbents in purification and depollution applications [3] [9] as well as catalyst supports [13] [14]. As the raw materials show differences in composition (carbon percentage), they do not behave the same way towards the activating agents and/or the temperature. The nature of biomass has thus a major impact on the characteristics of the end product.

The shell of *Parinari macrophylla* is a waste hardly biodegradable which represents an environment problem. *Parinari macrophylla* (a.k.a. *Neocarya macrophylla* or cayor apple tree) is a tree whose height ranges from 6 m to 10 m. It belongs to the *Chrysobalancea* family and to the *Parinari* genus. The plant is native to West and Central Africa [15] [16] [17]. This study aims to valorize these shells by producing active carbons. We intend to optimize the activation procedure and to characterize the end products regarding their adsorption capacities, their specific surfaces areas and their porous textures. The use of this raw material meets two goals, producing cheap quality AC from local agro-sourced material and valorizing wastes so that they gain an added value [7].

## 2. Materials and Methods

### 2.1. Production of the Active Carbons

The *Parinari macrophylla* (PM) shells were ground and sieved. The active carbons were produced using the granulometric fraction ranging from 2.5 mm to 5 mm.

#### 2.1.1. Physical Activation

The physical activation was carried out in a horizontal furnace (Lenton Thermal Design, CSC 12/600H), under a flow of nitrogen or of carbon dioxide (80 mL/min). The temperature was slowly risen with a ramp of 5°C/min up to the final temperature of 800°C/min which was maintained for 2 hrs. During the heating, two temperature plateaus were kept at 150°C for 30 min. and at 400°C for 1 hr (**Figure 1**). The goal of the step at 150°C was to dry the biomass and was always performed under a flow of nitrogen. The flowing gas was changed to carbon dioxide, if needed, after this drying step. The step at 400°C was used to

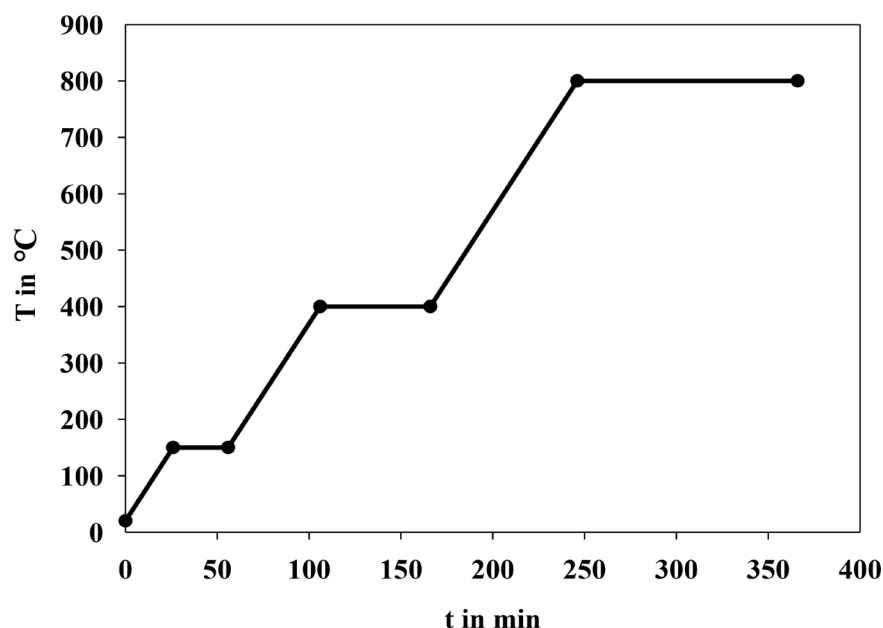


**Figure 1.** Temperature program for the pyrolysis (physical activations).

help the decomposition of the organic matter of the biomass. Its other purpose was to slow down the temperature rise, which is known to favour the production of more porous active carbons [18] [19] [20]. After the heating at 800°C, the furnace was let to cool down to room temperature, always under a flow of nitrogen.

Following the same operating conditions, as described above, we have produced charcoals physically activated by  $N_2/H_2O$  and  $CO_2/H_2O$  mixes. The main gas ( $N_2$  or  $CO_2$ ) passed, at room temperature, through a water flask, set up at the entrance of the furnace. Water vapors are thus driven into the furnace by the nitrogen or the carbon dioxide. The water flask was also heated in a thermostatic bath at 45°C and 70°C to increase the amount of water driven into the furnace by the activating gas.

Samples are identified as follows: Ph- (for physical activation) - $N_2$  or - $CO_2$ , depending on the activating gas, - $H_2O$  (X°C), if the activating gas passed through the water flask, heated at the temperature put in brackets (if no temperature is specified, the water flask is at room temperature). For instance, the sample activated under  $CO_2$  moisturized through a water flask at 45°C is noted Ph- $CO_2/H_2O$  (45°C).

### 2.1.2. Chemical Activation

The chemical activation consisted in two steps: the impregnation of orthophosphoric acid and the pyrolysis. The ground biomass was put into contact with  $H_3PO_4$ , with a ratio biomass (g)/acid solution (mL) of 1:3 wt/vol. The reference conditions were a  $H_3PO_4$  concentration of 5 mol/L, an impregnation time of 24 hrs, a pyrolysis temperature of 450°C and a pyrolysis time of 1.5 hr. After the impregnation, the samples were filtered and dried overnight at 110°C. The

pyrolysis was carried out in a chamber furnace (Heraeus). The temperature ramp was set to 10°C/min. After the pyrolysis, the samples were thoroughly washed with deionised water in a Soxhlet extractor, until the pH of the water, in contact with the sample, reached a value of 7. We have studied the effect of different H<sub>3</sub>PO<sub>4</sub> concentrations, impregnation times and pyrolysis temperatures and times (**Table 1**).

Samples are identified as follows: Ch (for chemical activation)-value for concentration of H<sub>3</sub>PO<sub>4</sub>-impregnation time-pyrolysis temperature-duration of final plateau. For instance, the sample, noted Ch-7M-450°C-1.5h, refers to the A.C. activated by H<sub>3</sub>PO<sub>4</sub> 7 mol/L, in the basic conditions of impregnation time and pyrolysis temperature and time (24 hrs, 450°C and 1.5 hr respectively).

### 2.1.3. Mixed Activation

The mixed activation consists in the impregnation of a chemical activating agent (H<sub>3</sub>PO<sub>4</sub>), followed by a pyrolysis, carried out in the same conditions as a physical activation.

We have studied the 24 hrs impregnation of the orthophosphoric acid at three concentrations (1.5 mol/L, 3 mol/L and 5 mol/L). As for the chemical activation, the ground biomass was put into contact with H<sub>3</sub>PO<sub>4</sub>, with a ratio biomass (g)/acid solution (mL) of 1:3. After the impregnation, the samples were filtered and dried overnight at 110°C. The pyrolysis was carried out following the same procedure as the physical activation, described above. The A.C. thus obtained were thoroughly washed with deionised water in a Soxhlet extractor, until the pH of the water, in contact with the sample, reached a value of 7.

Samples are identified as follows: Mx (for mixed activation)-H<sub>3</sub>PO<sub>4</sub> as the chemical activating agent (H<sub>3</sub>PO<sub>4</sub> concentration)-pyrolysis gas (N<sub>2</sub> or CO<sub>2</sub>). For

**Table 1.** Production conditions of A.C. through chemical activations.

[H <sub>3</sub> PO <sub>4</sub> ] (mol/L)	Impregnation time (h)	Pyrolysis temperature (°C)	Duration of final plateau (h)	Sample full name
5	24	450	1.5	Ch-5M-24 h-450°C-1.5 h
5	18	450	1.5	Ch-5M-18 h-450°C-1.5 h
5	12	450	1.5	Ch-5M-12 h-450°C-1.5 h
3.5	24	450	1.5	Ch-3.5M-24 h-450°C-1.5 h
7	24	450	1.5	Ch-7M-24 h-450°C-1.5 h
8.7	24	450	1.5	Ch-8.7M-24 h-450°C-1.5 h
5	24	300	1.5	Ch-5M-24 h-300°C-1.5 h
5	24	400	1.5	Ch-5M-24 h-400°C-1.5 h
5	24	500	1.5	Ch-5M-24 h-500°C-1.5 h
5	24	450	1	Ch-5M-24 h-450°C-1 h
5	24	450	2	Ch-5M-24 h-450°C-2 h
5	24	450	3	Ch-5M-24 h-450°C-3 h

instance, Mx-H<sub>3</sub>PO<sub>4</sub> (1.5M)-N<sub>2</sub> refers to the sample impregnated by H<sub>3</sub>PO<sub>4</sub> 1.5M, whose pyrolysis was performed under a flow of nitrogen.

## 2.2. Characterizations of the Active Carbons

### 2.2.1. Mass Yield of the Pyrolysis

The pyrolysis yield ( $y$ ) is related to the activation mode and to the source material. It is defined as the ratio between the final A.C. mass ( $m_f$ ) and the initial mass of the biomass ( $m_i$ ). The mass loss, caused by the activation process, also called burn-off, is given in Equation (1). The sum of the yield and the burn-off (in %) equals 100%.

$$\text{burn-off} = \frac{m_i - m_f}{m_i} \times 100 = 100 - y(\%). \quad (1)$$

### 2.2.2. Iodine Number

The adsorption capacity of active carbons may be evaluated through their iodine numbers. The iodine number measures the quantity of iodine (in mg) adsorbed by 1 g of the A.C., in fixed conditions. The method used in this work is based on the ASTM norm D4607-94 [21]. The sample is firstly boiled for 30 seconds in 10 mL HCl 5% to get rid of any sulfur compounds that might be present in the solid and that would interfere with the analysis. 100 mL of I<sub>2</sub> 0.1 N is then put into contact with the sample during 30 seconds and the suspension is filtered immediately. The iodine in the filtrate is titrated by a solution of sodium thiosulfate 0.1 N. Normally, the ASTM norm requires the titration of the residual iodine after adsorption on 3 different masses of sample. The iodine number is, by definition, the quantity of adsorbed iodine (in mg/g) corresponding to a residual iodine concentration of 0.02 N. Nevertheless, it does exist tables that give the iodine number based on the volume of thiosulfate necessary to titrate the residual iodine after adsorption on a single mass of solid. These tables exist for sample masses of 1 g, 1.5 g, 2 g and 3 g.

### 2.2.3. Nitrogen Adsorption at 77 K

The isotherms of the adsorption of nitrogen at 77 K were recorded using a Micromeritics Gemini VII device. The BET treatment of the isotherms led to the determination of the specific surface areas, the mean pore diameters and the total pore volumes (measured at  $P/P^\circ = 0.99$ ). The t-plot treatment of the data enabled the determination of the microporous surface areas and volumes.

## 3. Results and discussion

### 3.1. Mass Yield of the Pyrolysis

The mass yield ranges are presented, for the three activation modes, in **Table 2**. These results do not allow to prefer the physical activation over the other activation modes (mean yield of 25%). They show that the use of orthophosphoric acid as an activating agent increases the pyrolysis yield through a dehydration process. This delays the thermal decomposition of the raw material, thus limiting

**Table 2.** Ranges of mass yields and mass losses for physical, chemical and mixed activations. Values based on the weighing of the samples before and after the pyrolysis and computed following Equation (1).

	Physical activation	Chemical activation	Mixed activation
Mass yields (%)	23 - 28	31 - 45	31 - 37
Mass losses (burn-off) (%)	72 - 77	55 - 69	63 - 39

the loss of volatile matters, and it leads to a rigid carbonaceous matrix, as stated by Zhao *et al.* [22]. In the case of the chemical activation, a decrease of the pyrolysis yields is logically observed when the temperatures get higher (from 45% at 300°C to 38% at 400°C and 34% at 500°C, all other parameters being held at their reference values).

### 3.2. Iodine Number

The A.C. adsorption capacity, including the microporosity, in a condensed phase (aqueous) is estimated through the iodine number. Figure 2 shows the iodine numbers for the A.C. produced by physical activation. The physical activations under a flow of N<sub>2</sub> lead to low values of iodine numbers (between 131 mg I<sub>2</sub>/g and 193 mg I<sub>2</sub>/g). Moreover, the iodine number values of 200 mg I<sub>2</sub>/g and less are largely under the application range of the norm. The only conclusion that can be drawn is that the produced solids actually develop some porosity but cannot be referred to as proper active carbons. The addition of water vapors to the process does not change the adsorption capacity of the solids. The only value that significantly varies from the other ones is the iodine number corresponding to the solid obtained when the water is heated at 70°C. Not much can be concluded from this fact, as it might be a simple variation related to the lack of accuracy going along with the determination of iodine numbers lower than 200 mg I<sub>2</sub>/g. The physical activations under a flow of CO<sub>2</sub>, on the other hand, lead to higher values of iodine numbers and the higher the water vapor content, depending on the temperature of the water flask, the lower the iodine number. Thus, water has a negative effect on the iodine number value, during the physical carbonic activation.

Concerning the chemical activation with H<sub>3</sub>PO<sub>4</sub>, the iodine number rises with the increase of the acid concentration, the impregnation time and the pyrolysis temperature and time. When these parameters are set at their lowest, the iodine number is 256 mg I<sub>2</sub>/g and has been raised up to 457 mg I<sub>2</sub>/g (Figure 3). The effect of the orthophosphoric acid concentration on the iodine number has been observed during the mixed activations as well (Figure 4).

These results show that, whatever the activation mode, the microporosity of the active carbons obtained from *Parinari macrophylla* is always more developed when the medium is oxidative (CO<sub>2</sub>, H<sub>3</sub>PO<sub>4</sub>), which is confirmed by the lower iodine numbers in the presence of water vapors. Indeed, when the activation occurs under a mixed flow of CO<sub>2</sub>/H<sub>2</sub>O, the iodine numbers decrease proportionally

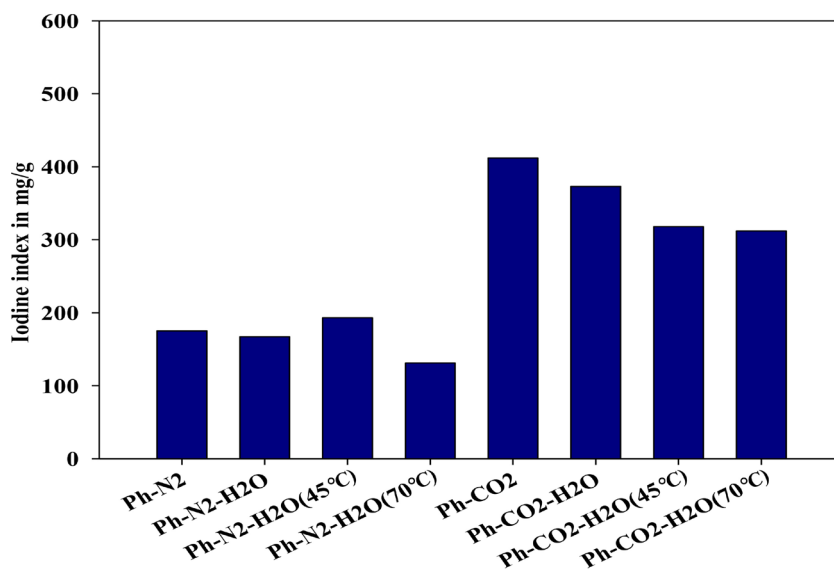


**Figure 2.** Iodine numbers of the A.C. produced by physical activations.

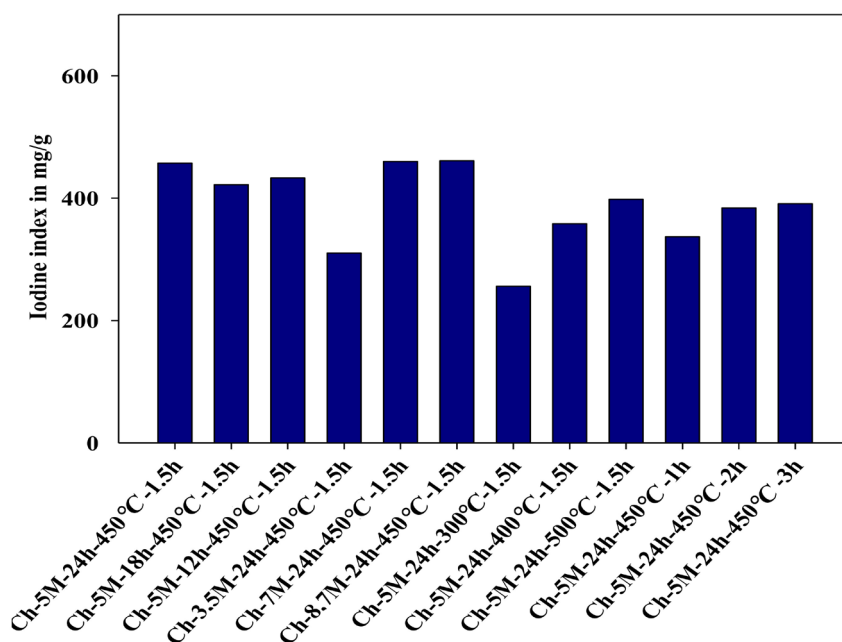


**Figure 3.** Iodine numbers of the A.C. produced by chemical activations.

with the amount of water vapors present in the pyrolysis reactor (depending on the temperature of the water through which the CO<sub>2</sub> is flowing to moisturize it). This shows that water vapors interfere with the action of CO<sub>2</sub> during the creation process of the porosity. On the other hand, the presence of water, during the activations under N<sub>2</sub> flow, shows little to no impact on the iodine numbers. This leads to think that water vapors are involved, in the physical activation process under CO<sub>2</sub> flow, either by inhibiting the creation of pores or by boosting the creation of meso- and macropores, which would also decrease the iodine number values.

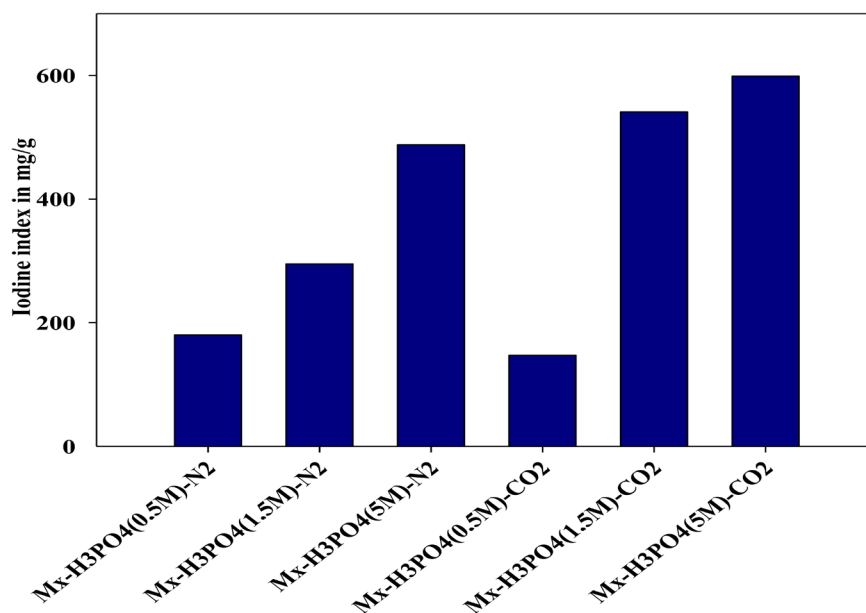


**Figure 4.** Iodine numbers of the A.C. produced by mixed activations.

The influence of the orthophosphoric acid concentration has been reported about the activation of several biomasses [5] [23]. It has been shown that this acid increases the microporosity adsorption capacity (as shown in this work as well) up to a certain concentration or a certain H<sub>3</sub>PO<sub>4</sub> mass ratio, above which the medium becomes too oxidative and leads to the destruction of the porous network. This concentration limit in H<sub>3</sub>PO<sub>4</sub> depends, of course, on the nature of the source material.

Concerning the activations in the presence of H<sub>3</sub>PO<sub>4</sub> (chemical and mixed), the increase of its concentration produces A.C. with higher iodine numbers (Figure 3 and Figure 4). The effect is particularly obvious in the case of mixed activations, as the increase of H<sub>3</sub>PO<sub>4</sub> concentration, from 0.5 mol/L to 5 mol/L, leads to a rise of the iodine numbers of 300 mg/g when the pyrolysis occurs under N<sub>2</sub> and of 450 mg/g when the pyrolysis occurs under CO<sub>2</sub>. It is worth to note that the mixed activations give the A.C. with the highest adsorption capacities towards iodine.

### 3.3. Nitrogen Adsorption at 77 K

The nitrogen adsorption at 77 K has enabled to determine the BET specific surface area, BET microporous surface area, total and microporous volumes of the produced A.C. All these characteristics are listed in Table 3.

During physical activations, the specific surface area values are too low for proper active carbons (less than 450 m<sup>2</sup>/g), which is consistent with the low iodine number values exhibited by those solids. Nevertheless, the analysis of the BET isotherms proves that an internal (thus porous) surface has been developed during the process. The specific surface areas globally decrease as water vapors are added to the medium, going down from 315 m<sup>2</sup>/g (entry 3) to 171 m<sup>2</sup>/g

**Table 3.** Specific surface areas, microporous surfaces, total pore volumes, micropore volumes and mean pore diameters of A.C. produced by physical, chemical and mixed activations.

Entry	Sample full name	S <sub>BET</sub> (m <sup>2</sup> /g)	S <sub>micro</sub> (m <sup>2</sup> /g)	S <sub>micro</sub> /S <sub>BET</sub>	V <sub>total</sub> (cm <sup>3</sup> /g)	V <sub>micro</sub> (cm <sup>3</sup> /g)	V <sub>micro</sub> /V <sub>total</sub>	d <sub>moyen</sub> (Å)
Physical activation								
1	Ph-N <sub>2</sub>	298	193	0.646	0.140	0.073	0.520	19
2	Ph-N <sub>2</sub> -H <sub>2</sub> O	266	188	0.708	0.125	0.071	0.569	19
3	Ph-N <sub>2</sub> -H <sub>2</sub> O (45°C)	315	199	0.632	0.146	0.074	0.508	19
4	Ph-N <sub>2</sub> -H <sub>2</sub> O (70°C)	171	62	0.359	0.097	0.028	0.293	23
5	Ph-CO <sub>2</sub>	454	362	0.798	0.220	0.142	0.648	19
6	Ph-CO <sub>2</sub> -H <sub>2</sub> O	447	344	0.769	0.209	0.135	0.648	19
7	Ph-CO <sub>2</sub> -H <sub>2</sub> O (45°C)	312	195	0.625	0.169	0.074	0.435	22
8	Ph-CO <sub>2</sub> -H <sub>2</sub> O (70°C)	408	301	0.738	0.202	0.117	0.579	20
Chemical activation								
9	C h-5M-24 h-450°C-1.5 h	727	627	0.863	0.306	0.245	0.799	17
10	C h-5M-18 h-450°C-1.5 h	621	526	0.847	0.266	0.206	0.774	17
11	C h-5M-12 h-450°C-1.5 h	614	519	0.845	0.263	0.203	0.772	17
12	C h-3.5M-24 h-450°C-1.5 h	381	283	0.743	0.175	0.110	0.633	18
13	C h-7M-24 h-450°C-1.5 h	627	537	0.856	0.265	0.209	0.790	17
14	C h-8.7M-24 h-450°C-1.5 h	633	536	0.847	0.273	0.209	0.768	17
15	C h-5M-24 h-300°C-1.5 h	331	260	0.785	0.150	0.102	0.683	18
16	C h-5M-24 h-400°C-1.5 h	417	337	0.808	0.185	0.132	0.715	18
17	C h-5M-24 h-500°C-1.5 h	557	474	0.851	0.239	0.185	0.776	17
18	C h-5M-24 h-450°C-1 h	454	372	0.819	0.198	0.146	0.734	17
19	C h-5M-24 h-450°C-2 h	455	381	0.837	0.197	0.149	0.755	17
20	C h-5M-24 h-450°C-3 h	534	453	0.848	0.229	0.177	0.773	17
Mixed activation								
21	Mx-H <sub>3</sub> PO <sub>4</sub> (0.5M)-N <sub>2</sub>	355	250	0.704	0.160	0.096	0.601	18
22	Mx-H <sub>3</sub> PO <sub>4</sub> (1.5M)-N <sub>2</sub>	441	360	0.818	0.201	0.146	0.725	18
23	Mx-H <sub>3</sub> PO <sub>4</sub> (5M)-N <sub>2</sub>	575	510	0.887	0.251	0.205	0.816	17
24	Mx-H <sub>3</sub> PO <sub>4</sub> (0.5M)-CO <sub>2</sub>	207	106	0.514	0.104	0.042	0.403	20
25	Mx-H <sub>3</sub> PO <sub>4</sub> (1.5M)-CO <sub>2</sub>	608	537	0.884	0.256	0.210	0.821	17
26	Mx-H <sub>3</sub> PO <sub>4</sub> (5M)-CO <sub>2</sub>	658	578	0.878	0.275	0.225	0.819	17

(entry 4) under nitrogen and from 447 m<sup>2</sup>/g (entry 6) to 408 m<sup>2</sup>/g (entry 8) under carbon dioxide. When carbon dioxide is used on its own, this leads to a more porous solid, developing more surface area, than when nitrogen is used alone (see entry 5 vs. entry 1). This fact could be due to the oxidizing properties of CO<sub>2</sub>, which are favorable for the creation of pores during the pyrolysis of the biomass. The microporous surface and microporous volume follow the same decreasing trend. The presence of water vapors seems to lead to a less microporous volume under N<sub>2</sub> (ratio V<sub>micro</sub>/V<sub>total</sub> is lower with water at 45°C or 70°C,

see **entries 3 and 4**) and a more microporous volume under CO<sub>2</sub> (ratio  $V_{\text{micro}}/V_{\text{total}}$  is higher with at 45°C or 70°C, see **entries 7 and 8**). The pore diameters follow the same order of evolution.

When the chemical activation with H<sub>3</sub>PO<sub>4</sub> is studied, the specific surface area ranges from 331 m<sup>2</sup>/g (**entry 15**) to 727 m<sup>2</sup>/g (**entry 9**) and rises with the increase of the H<sub>3</sub>PO<sub>4</sub> concentration (**entries 12, 13 and 14**), the impregnation time (**entries 11, 10 and 9**) and the pyrolysis temperature (**entries 15, 16 and 17**) and time (**entries 18, 13 and 14**). The micropores remain the major porosity type of all the A.C. produced, even for the solids with the lowest specific surface areas (**entries 12 and 15**). Indeed, all the chemically activated carbons display a microporous surface area representing more than 74% of the total area, a microporous volume representing more than 63% (sample which has the lowest porosity is **entry 12**) of the total pore volume and a mean pore diameter lower than 20 Å.

The same observations can be made for the mixed activations when considering the phosphoric acid concentrations (**entries 21, 22 and 23** as well as **entries 24, 25 and 26**). Excepted for the lowest phosphoric concentration, nitrogen seems to lead to lower specific surface areas than carbon dioxide (**entries 22 vs. 25** as well as **entries 23 vs. 26**). Microporous surface and microporous volumes are often, higher than 80%. This activation mode has allowed to produce active carbons displaying specific surface area values similar to the values obtained for the A.C. produce by chemical activation, but while using lower concentrations in H<sub>3</sub>PO<sub>4</sub>. It is to be noted that the mixed activations, using CO<sub>2</sub>, give A.C. with higher specific surface areas than when N<sub>2</sub> is used. Chemical and mixed activations generally lead to active carbons with similar porosities whereas the ones produced by physical activation rather develop a lower porosity. Indeed, the orthophosphoric acid, used during the chemical and mixed activations, plays a major role in the pore formation. It takes part in the depolymerization reactions involving the macromolecules of the biomass (degraded in CO, CO<sub>2</sub> and CH<sub>4</sub>), as well as in the condensation and cyclization reactions of the polyaromatic structures [24], which lead to the formation of a porous and rigid carbonaceous material. On the contrary, during the physical activation, the reactions at high temperature (up to 800°C), under flows of CO<sub>2</sub> or N<sub>2</sub> alone, do not allow to get the same level of pore formation [24]. Furthermore, it is to be noted that the best active carbons, produced from the pyrolysis of *Parinari macrophylla* shells, have characteristics similar to these of some active carbons produced from others agricultural wastes [1] [2] [12] [20] [25] and of some commercial active carbons, which have generally higher pore volumes though (frequently close to 0.4 cm<sup>3</sup>/g or higher, while the active carbons produced for this work reach 0.3 cm<sup>3</sup>/g at best). For instance, the active carbon supplied by Merck (ref. 2184) show a specific surface area of 469 m<sup>2</sup>/g and a pore volume of 0.38 cm<sup>3</sup>/g, or the active carbon Lurgi Hydradin show a specific surface area of 762 m<sup>2</sup>/g and a pore volume of 0.40 cm<sup>3</sup>/g.

Nevertheless, the nature of the pyrolysis gas has no effect on the percentage of

microporous surface area and volume. This may mean that the microporosity is essentially due to  $H_3PO_4$ . These results show an opposite effect of water and orthophosphoric acid on the microporosity of the final A.C. Water tends to decrease the microporosity of the A.C. while  $H_3PO_4$  increases it. In the production of A.C. from *Parinari macrophylla*, the studied activating agents contribute to the creation of microporosity in the following order:  $N_2 < CO_2 < H_3PO_4$ . The increase of the amount of these activating agents in the medium leads to higher specific surface areas [5] [8] [25] [26] [27].

### 3.4. Relation between the Iodine Number and the BET Specific Surface Area

Globally, the iodine numbers change alongside the BET surface areas. Although the two measures do not characterize exactly the same property of the solids, they both give an indication of the adsorption capacity for small size molecules. Indeed, both analyses are based on the adsorption of small molecules,  $N_2$  having a molecular radius of 2.1 Å and a cross-sectional area of 16.2 Å<sup>2</sup>, and  $I_2$  having a molecular radius of 3.3 Å and a cross-sectional area of 22.6 Å<sup>2</sup>. These dimensions give them a good accessibility to the majority of the active carbon porosity, including the microporosity (pore diameters lower than 20 Å) despite the fact that the  $N_2$  adsorption occurs in gas phase and the  $I_2$  adsorption occurs in condensed aqueous phase.

It is thus legit and interesting to plot the graph of specific surface area vs iodine number and micropore surface area vs iodine number. These plots are presented in Figures 5-7 for the A.C. produced by physical, chemical and mixed activations, respectively.

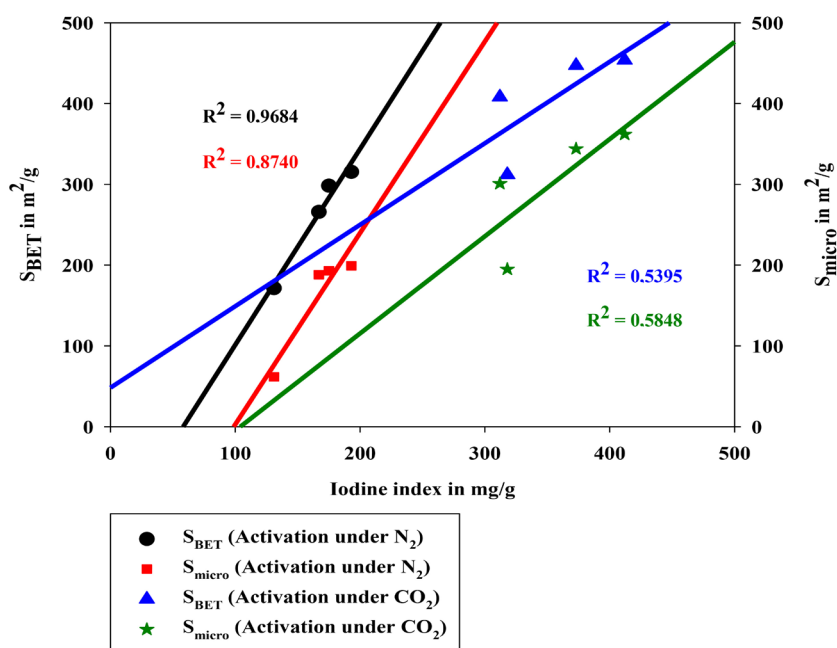


**Figure 5.** Relation between the iodine number and the specific surface area or the microporous surface for A.C. produced by physical activations.

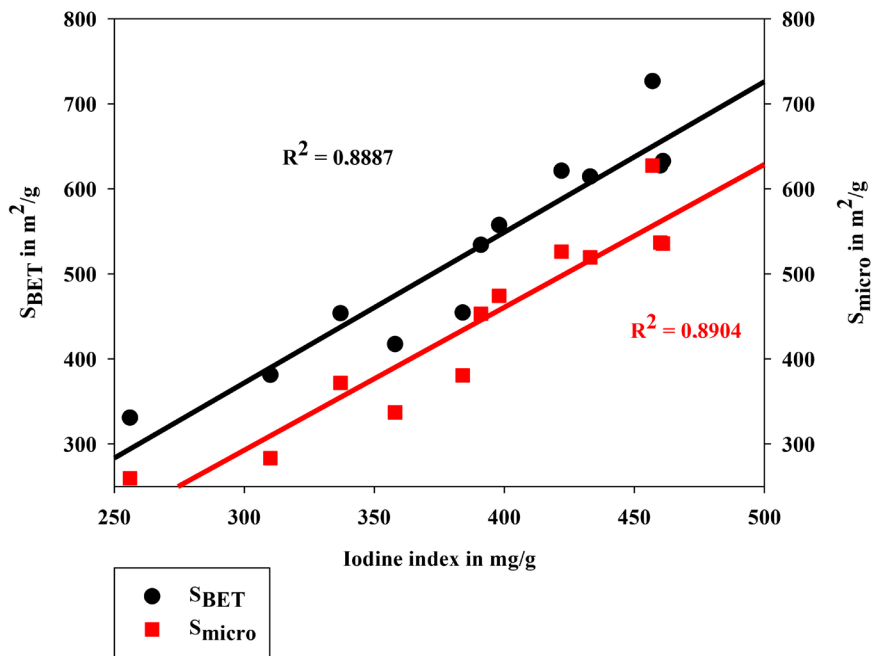


**Figure 6.** Relation between the iodine number and the specific surface area or the microporous surface for A.C. produced by chemical activations.

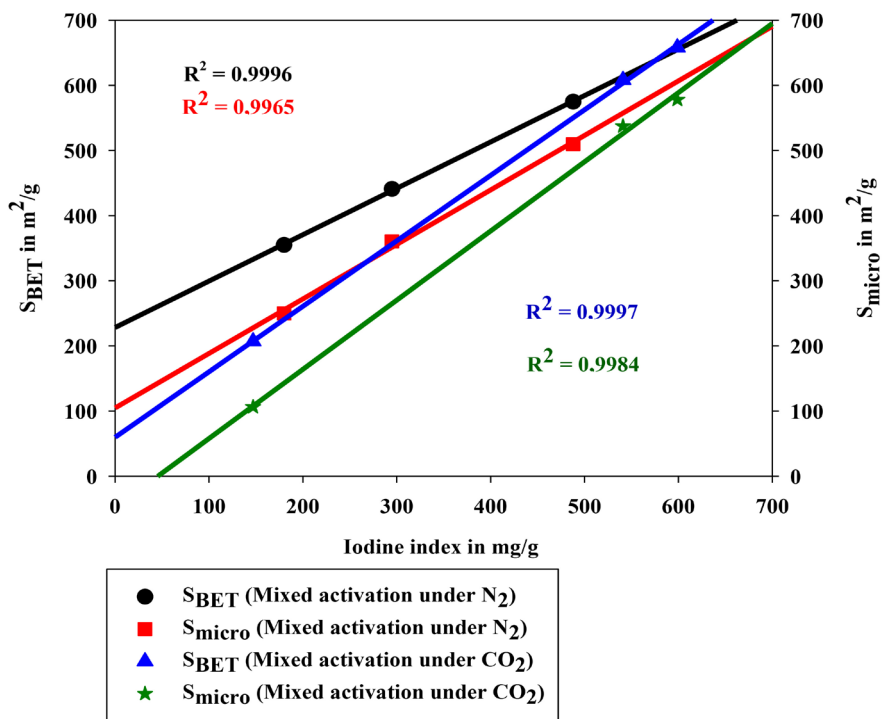


**Figure 7.** Relation between the iodine number and the specific surface area or the microporous surface for A.C. produced by mixed activations.

A linear trend can be observed between the iodine number and the surface area values and is validated by the correlation coefficient ( $r^2$ ) of the linear regression, which usually ranges from 0.8740 to 0.9996. The  $r^2$  values for the graphs

“surface area (total or microporous) vs iodine number” are low (0.5395 to 0.5848) in the case of A.C. produced by CO<sub>2</sub> physical activation. These low r<sup>2</sup> are nevertheless obtained for regressions performed on only four points. All it takes for r<sup>2</sup> to drop is one-point diverging from the regression line, which is the case here, as two A.C. with similar iodine numbers exhibit different surface areas. For chemical activations, the same phenomenon of different surface areas corresponding to similar iodine numbers can be observed for a couple of A.C. (iodine number around 460 mg I<sub>2</sub>/g) but as the regression curves are plotted on a dozen points, the r<sup>2</sup> are still about 0.8903.

For a given activation mode, the linear regressions “total surface area vs iodine number” and “micropore surface area vs iodine number” are basically parallel, which indicates that there is, as well, a good correlation between the specific surface area and the micropore surface area. It is thus possible to estimate, roughly, the specific surface area or the iodine number if the other one is known, and it is also possible to estimate the micropore surface area from either the total surface area or the iodine number.

### 3.5. Relation between the Pyrolysis Yield, the Iodine Number and the Specific Surface Area

The porosity of the A.C. is created simultaneously with the decomposition of the biomass, during the pyrolysis and the activation processes. In the case of *Parinari macrophylla* as the source material, the production of the A.C. goes along with a mass loss of 55% to 77%, corresponding to pyrolysis yields of 45% and 23% respectively (**Table 2**). However, the highest values of surface area or iodine number are not connected to the highest mass losses, and this observation is true for all the activation modes.

Moreover, the chemical activation with H<sub>3</sub>PO<sub>4</sub> leads to higher values of specific surface areas and iodine numbers, albeit with a higher pyrolysis yield (thus less mass loss), than the physical activation. This confirms that the orthophosphoric acid, as an activating agent, delays the decomposition of the biomass while it contributes to the formation of a rigid carbonaceous network [22], which can be explained by the creation of P-O-C bonds [12] [28] [29]. H<sub>3</sub>PO<sub>4</sub> hence takes part in the biomass decomposition and also in the pore creation process. Marsh and Rodriguez-Reinoso [24] have suggested a reaction mechanism for the effect of H<sub>3</sub>PO<sub>4</sub> on lignocellulosic biomass. It implies the formation of phosphoric acid esters at temperatures lower than 450°C, the elimination of the acid at temperatures above 450°C and the creation of ink bottle shaped pores as H<sub>3</sub>PO<sub>4</sub> is released. However, a fraction of the acid remains in the A.C., as proved by the presence of FTIR signals corresponding to P-O-C bonds.

## 4. Conclusions

The present study proves that one can produce active carbons from *Parinari macrophylla* shells. The analysis of the isotherms of nitrogen adsorption shows

that these active carbons are essentially microporous.

At this stage of the research, the solids obtained by physical activation alone are not really interesting, although they develop some porosity. Indeed, they show the lower pyrolysis yields and their specific surface areas, as well as their iodine numbers, are too low to consider them as proper active carbons.

Concerning the chemical activation, this method has given the porous solids displaying the highest specific surface areas, iodine numbers and pore volumes, characteristics that fit more what can be expected from active carbons. However, a major drawback of this activation mode is the use of chemicals (orthophosphoric acid in this case), often at high concentration, which can be harmful to the environment and to the properties of the active carbon surface.

The mixed activation has led to obtain porous solids with physico-chemical properties similar to the ones observed after chemical activations, but with the benefit of using a more dilute activating agent. Therefore, it would be worthwhile to carry on investigating this activation method.

The usefulness of the active carbons prepared from *Parinari macrophylla* shells has to be evaluated through their performances as adsorbents or as catalyst supports. This could be of high economic and ecological interest as this could be an outlet to recycle an agricultural waste.

## Acknowledgements

Special thanks to Vincent Dubois for making possible the collaboration between Labiris (Brussels, Belgium) and the Abdou Moumouni University of Niamey (Niger). The authors would also like to thank Moussa Barag , Philippe Donnen, Pierre Martinot and Julie Sepulchre for organizing the ARES support and internship in Belgium.

## Conflicts of Interest

The authors declare no conflicts of interest regarding the publication of this paper.

## References

- [1] Jagiello, J., Kenvin, J., Celzard, A. and Fierro V. (2019) Enhanced Resolution of Ultra-Micropore Size Determination of Biochars and Activated Carbons by Dual Gas Analysis Using N<sub>2</sub> and CO<sub>2</sub> with 2D-NLDFT Adsorption Models. *Carbon*, **144**, 206-215. <https://doi.org/10.1016/j.carbon.2018.12.028>
- [2] Sekirifa, M.L., Hadj-Mahammed, M., Pallier, S., Baameur, L., Richard, D. and ADujaili, A.H. (2013) Preparation and Characterization of an Activated Carbon from a Date Stones Variety by Physical Activation with Carbon Dioxide. *Journal of Analytical and Applied Pyrolysis*, **99**, 155-160. <https://doi.org/10.1016/j.jaap.2012.10.007>
- [3] Di m , M.M., Hervy, M., Diop, S.N., G rente, C., Villot, A., Andres, Y. and Diawara, C.K. (2016) Sustainable Conversion of Agriculture and Food Waste into Activated Carbons Devoted to Fluoride Removal from Drinking Water in Senegal. *International Journal of Chemistry*, **8**, 8-15. <https://doi.org/10.5539/ijc.v8n1p8>

- [4] Zaini, M.A.A., Zhi, L.L., Hui, T.S., Amano, Y. and Machida, M. (2021) Effects of Physical Activation on Pore Textures and Heavy Metals Removal of Fiber-Based Activated Carbons. *Materialstoday Today: Proceedings*, **39**, 917-921. <https://doi.org/10.1016/j.matpr.2020.03.815>
- [5] Balogoun, C.K., Bawa, M.L., Osseni, S. and Aina, M. (2015) Préparation des charbons actifs par voie chimique à l'acide phosphorique à base de coque de noix de coco. *International Journal of Biological and Chemical Sciences*, **9**, 563-580. <https://doi.org/10.4314/ijbcs.v9i1.48>
- [6] Gnosoro, U.P., Yao, K.M., Yao, B.L., Kouassi, A.M., Dembélé, A., Kouakou, Y.U., Ouattara, K.P.H., Diabaté, D. and Trokourey, A. (2015) Adsorption du benzo(a)pyrène sur du charbon activé à base de coques de coco provenant de Côte d'Ivoire. *International Journal of Biological and Chemical Sciences*, **9**, 2701-2711. <https://doi.org/10.4314/ijbcs.v9i5.39>
- [7] Mamane, O.S., Zanguina, A., Daou, I. and Natatou, I. (2016) Préparation et caractérisation de charbons actifs à base de coques de noyaux de Balanites Egypitiaca et de Zizyphus Mauritiana. *Journal de la Société Ouest-Africaine de Chimie*, **41**, 59-67.
- [8] Reffas, A., Bernardet, V., David, B., Reinert, L., Bencheikh Lehocine, M., Dubois, M., Batisse, N. and Duclaux, L. (2010) Carbons Prepared from Coffee Grounds by H<sub>3</sub>PO<sub>4</sub> Activation: Characterization and Adsorption of Methylene Blue and Nylosan Red N-2RBL. *Journal of Hazardous Materials*, **175**, 779-788. <https://doi.org/10.1016/j.jhazmat.2009.10.076>
- [9] Liou, T.-H. (2010) Development of Mesoporous Structure and High Adsorption Capacity of Biomass-Based Activated Carbon by Phosphoric Acid and Zinc Chloride Activation. *Chemical Engineering Journal*, **158**, 129-142. <https://doi.org/10.1016/j.cej.2009.12.016>
- [10] Williams, P.T. and Reed, A.R. (2006) Development of Activated Carbon Pore Structure via Physical and Chemical Activation of Biomass Fibre Waste. *Biomass Bioenergy*, **30**, 144-152. <https://doi.org/10.1016/j.biombioe.2005.11.006>
- [11] Ashfaq, A., Hassan, M.A.S. and Ahmad, H.A. (2015) Production of Activated Carbon from Raw Date Palm Fronds by ZnCl<sub>2</sub> Activation. *Journal of The Chemical Society of Pakistan*, **37**, 1081-1087.
- [12] Danish, M., Hashim, R., Ibrahim, M.N.M. and Sulaiman, O. (2014) Optimized Preparation for Large Surface Area Activated Carbon from Date (*Phoenix dactylifera* L.) Stone Biomass. *Biomass and Bioenergy*, **61**, 167-178. <https://doi.org/10.1016/j.biombioe.2013.12.008>
- [13] Bouchenafa-Saib, N., Grange, P., Verhasselt, P., Addoun, F. and Dubois, V. (2005) Effect of Oxidant Treatment of Date Pit Active Carbons Used as Pd Supports in Catalytic Hydrogenation of Nitrobenzene. *Applied Catalysis A: General*, **286**, 167-174. <https://doi.org/10.1016/j.apcata.2005.02.022>
- [14] Hermans, S., Diverchy, C. and Dubois, V. (2014) Pd Nanoparticles Prepared by Grafting of Pd Complexes on Phenol-Functionalized Carbon Supports for Liquid Phase Catalytic Applications. *Applied Catalysis A: General*, **474**, 263-271. <https://doi.org/10.1016/j.apcata.2013.09.029>
- [15] Dan Guimbo, I., Ambouta, K.J.M., Mahamane, A. and Larwanou, M. (2011) Germination et croissance initiale de *Neocarya macrophylla* (Sabine) Prance, une espèce oléagineuse du Niger. *Tropicultura*, **29**, 88-93.
- [16] Dan Guimbo, I., Laouali, A., Habou, R., Mahamane, A. and Ambouta, K.J.M. (2017) Le Pommier de Cayor, Espece Emblematique du Dallol Bosso (NIGER) Agron.

- Africaine*, **29**, 13-19.
- [17] Balde, M. (2018) Etude physico-chimique et valorisation de composés bioactifs de *Parinari macrophylla* Sabine (Chrysobalanaceae). Thèse de doctorat. Université de Strasbourg et Université Cheikh Anta Diop de Dakar.
- [18] Raveendran, K. and Ganesh, A. (1998) Adsorption Characteristics and Pore-Development of Biomass-Pyrolysis Char. *Fuel*, **77**, 769-781.  
[https://doi.org/10.1016/S0016-2361\(97\)00246-9](https://doi.org/10.1016/S0016-2361(97)00246-9)
- [19] Yang, H., Yan, R., Chen, H., Lee, D.H. and Zheng, C. (2007) Characteristics of Hem-cellulose, Cellulose and Lignin Pyrolysis. *Energy & Fuels*, **86**, 1781-1788.  
<https://doi.org/10.1016/j.fuel.2006.12.013>
- [20] Mamane, S.O., Siragi Dounounou, B.M., Malam Alma, M.M. and Natatou I. (2018) Valorisation des coques de noyaux de *Balanites aegyptiaca* (L.) Del. et *Hyphaene thébaïca* (L.) Mart. pour l'élaboration et caractérisation de Charbons Actifs; application pour l'élimination du chrome. *European Scientific Journal*, **14**, 195-216.  
<https://doi.org/10.19044/esj.2018.v14n21p195>
- [21] American Society for Testing and Materials (ASTM) (2006) Standard Test Method for Determination of Iodine Number of Activated Carbon. ASTM Standard D4607-94, ASTM International, West Conshohocken. <http://www.astm.org>
- [22] Zhao, J., Lai, C., Dai, Y. and Xie, J. (2007) Pore Structure Control of Mesoporous Carbon as Supercapacitor Material. *Materials Letters*, **61**, 4639-4642.  
<https://doi.org/10.1016/j.matlet.2007.02.071>
- [23] Tchakala, I., Bawa, L.M., Djaneye-Boundjou, G., Doni, K.S. and Nambo, P. (2012) Optimisation du procédé de préparation des Charbons Actifs par voie chimique ( $H_3PO_4$ ) à partir des tourteaux de Karité et des tourteaux de Coton. *International Journal of Biological and Chemical Sciences*, **6**, 461-478.  
<https://doi.org/10.4314/ijbcs.v6i1.42>
- [24] Marsh, H. and Rodríguez-Reinoso, F. (2006) Activated Carbon. Elsevier, Oxford.
- [25] Shofolahan, A.M., Agyei, N.M. and Okonkwo, J.O. (2016) Preparation, Characterization and Application of  $H_3PO_4$  Activated Maize Tassel for Remediation of Eutrophic Phosphorus. *Fresenius Environmental Bulletin*, **25**, 2514-2518.
- [26] Ma, M., Ying, H., Cao, F., Wang, Q. and Ai, N. (2020) Adsorption of Congo Red on Mesoporous Activated Carbon Prepared by  $CO_2$  Physical Activation. *Chinese Journal of Chemical Engineering*, **28**, 1069-1076.  
<https://doi.org/10.1016/j.cjche.2020.01.016>
- [27] Yang, T. and Lua, A.C. (2003) Characteristics of Activated Carbons Prepared from Pistachio-Nut Shells by Physical Activation. *Journal of Colloid and Interface Science*, **267**, 408-417. [https://doi.org/10.1016/S0021-9797\(03\)00689-1](https://doi.org/10.1016/S0021-9797(03)00689-1)
- [28] Gratuito, M.K.B., Panyathanmaporn, T., Chumnanklang, R.A., Sirinuntawittaya, N.B. and Dutta, A. (2008) Production of Activated Carbon from Coconut Shell: Optimization Using Response Surface Methodology. *Bioresource Technology*, **99**, 4887-4895. <https://doi.org/10.1016/j.biortech.2007.09.042>
- [29] Puziy, A.M., Poddubnaya, O.I., Martinez-Alonso, A., Suarez-Garcia, F. and Tascon, J.M.D. (2005) Surface Chemistry of Phosphorus-Containing Carbons of Lignocellulosic Origin. *Carbon*, **43**, 2857-2868. <https://doi.org/10.1016/j.carbon.2005.06.014>